Chemical Physics Letters 616–617 (2014) 137–141

Contents lists available at ScienceDirect

Chemical Physics Letters

journal homepage: www.elsevier.com/locate/cplett

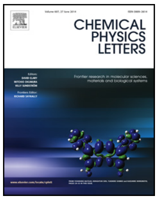

Unusually short excited state lifetimes of indenofluorene and fluorenofluorene derivatives result from a conical intersection

Bradley D. Rose[a], Leah E. Shoer[b], Michael R. Wasielewski[b], Michael M. Haley[a,*]

[a] *Department of Chemistry & Biochemistry and the Materials Science Institute, 1253 University of Oregon, Eugene, OR 97403-1253, United States*
[b] *Department of Chemistry and Argonne-Northwestern Solar Energy Research (ANSER) Center, Northwestern University, 2145 Sheridan Road, Evanston, IL 60208-3113, United States*

ARTICLE INFO

Article history:
Received 27 August 2014
In final form 14 October 2014
Available online 22 October 2014

ABSTRACT

The ultrafast excited state decay rates for indenofluorene and fluorenofluorene derivatives as measured by transient absorption spectroscopy are reported. The excited state lifetimes of the molecules were extremely short (ca. 9–12 ps) and are a result of the *p*-xylylene motif in indenofluorenes and the corresponding expanded 2,6-naphthoquinonedimethide in fluorenofluorene. Quantum chemical calculations indicate that the fast relaxation to the ground state results from a potential energy surface crossing between the S_0 and S_1 states. This process in turn provides an efficient route for excited state deactivation and explains why this class of quinoidal molecules is non-emissive.

1. Introduction

There has been much interest in materials for easily produced organic electronics [1]. Applications such as organic photovoltaics (OPVs) and field-effect transistors (OFETs) often require not only high efficiencies but also additional characteristics including processability, flexibility and photoactivity [2–4]. Numerous small-molecule systems have been developed toward this goal that employ extended pi-conjugated centers [5–9]. One such molecular class of interest is the *p*-quinodimethane-containing indenofluorenes and related molecules (e.g., **1**–**3**, Figure 1), which have recently been realized through synthesis [10–17]. Intriguingly, these compounds have been found to be non-emissive and thus we wished to examine their photophysics. One possible mechanism for non-emissive relaxation from a photoexcited state to the ground state is singlet fission, proposed to be present in the expanded system fluorenofluorene (**1**), due to ideal state energies for singlet fission [18]. This process is particularly desirable in OPVs as it may boost the maximum power conversion efficiency and impede loss pathways from charge recombination [19,20]. Another plausible mechanism for the lack of emission is internal conversion through a conical intersection between the ground state, S_0, and the singlet first excited state, S_1. Such a mechanism is the cause for efficient internal conversion in **4**, a substructure of **2** [21].

2. Experimental

2.1. Materials

All molecules were synthesized as previously reported [10,11,13].

2.2. Optical spectroscopy

Femtosecond transient absorption (fsTA) measurements were made using a regeneratively amplified Ti:sapphire laser system operating at 832 nm and a 1 kHz repetition rate as described previously [22–24]. Samples had an absorbance of 0.3–0.7 in dry toluene at the excitation wavelength of 495 nm and were irradiated in 2 mm quartz cuvettes with 1 μJ/pulse focused to a 0.2 mm diameter spot. The total instrument response function (IRF) was 180 fs. Transient spectra were averaged for 5 s. Kinetic traces corresponding to the ground state bleach and excited state absorption for each spectrum were fit using a Levenberg–Marquardt nonlinear least squares fit to a sum of exponentials convoluted with a Gaussian instrument response function.

---

* Corresponding author.
E-mail addresses: m-wasielewski@northwestern.edu (M.R. Wasielewski), haley@uoregon.edu (M.M. Haley).

http://dx.doi.org/10.1016/j.cplett.2014.10.031
0009-2614/

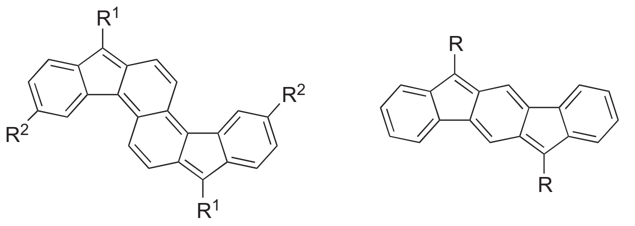

1a, R^1 = mesityl, R^2 = tert-butyl
1b, $R^1 = R^2$ = H

2a, R = (triisopropylsilyl)ethynyl
2b, R = H

3a, R = (triisopropylsilyl)ethynyl
3b, R = H

4

Figure 1. Structures of indenofluorene and fluorenofluorene derivatives investigated in this letter (**1**–**3**) as well as the structure of a related indenofluorene subunit, *s*-indacene (**4**).

2.3. Computational methods

Geometries were optimized using the fully optimized reaction space (FORS) method within the General Atomic and Molecular Electronic Structure System (GAMESS) package of programs [25]. This method can formally account for the static electronic correlation present in these systems. Further approximations are still needed to make this a manageable problem with presently available computational resources, so the pendant aryl/ethynyl groups were omitted and only a minimal active space was used—four electrons in four orbitals, denoted FORS(4,4). Single point energies were also computed using multiconfigurational quasidegenarate perturbation theory (MCQDPT2) [26]. The cc-pVDZ basis set [27] was used for all cases, except for TD-DFT where the 6-311G(2df,2p) basis set [28] was used; thus, all electronic ground state structures were minimized using FORS(4,4)/cc-pVDZ. In the case of the photoexcited states, state averaging was done with equal weights given to the S_0 and S_1 states, denoted SA-FORS(4,4). The S_0 and S_1 geometries were verified as stationary points by frequency analysis. No symmetry was enforced when searching for the conical intersections and the geometries were considered minimized when a maximum gradient of less than 0.0004 Hartree/bohr was located, as set by OPTTOL in GAMESS. Single point TD-DFT calculations were carried out using CAM-B3LYP [29,30]. Cartesian coordinates for structures are available as supplementary files named according to the scheme in text. The programs Macmolplt [31], Chemcraft [32], and CYLview [33] were used to generate and view structures. Considering the approximations used, the results obtained are only considered qualitatively correct as a larger active space, basis set and dynamic electron correlation would be needed for quantitatively correct results, but are beyond the scope and computational expense of this current study.

3. Results and discussion

The first system explored using transient absorption spectroscopy in solution was fluoreno[4,3-*c*]fluorene derivative **1a** [10]. The initial absorptive feature that appears at approximately 675–800 nm (Figure 2a) is likely related to the S_2 state, as the calculated S_0–S_1 transition is forbidden in this system (vide infra). Rapid internal conversion in less than a picosecond resulted in a blue-shifted absorptive feature corresponding to S_1, which significantly overlaps with the ground state bleach from 470 nm to 650 nm. This lowest-lying excited state then decays with the ultrashort lifetime of $\tau = 11.9 \pm 3.5$ ps (Figure 2b). Because the internal conversion from S_2 to S_1 occurs so quickly, it is difficult to resolve the spectral signature from the intrinsic chirp from the probe pulse, even utilizing global analyses like singular value decomposition (SVD). SVD is able to spectrally resolve a shift in the excited state from redder to bluer wavelengths that is associated with vibrational cooling processes (Figure S2); however, the rate of internal conversion from S_1 to S_0 is fast enough to be competitive with vibrational cooling, which complicates assignment of individual processes rates in single-wavelength kinetic fits where the cooling can be observed (i.e., red of the S_1 absorption maximum).

We also studied the related but smaller derivatives indeno[1,2-*b*]fluorene (**2a**) [13] and indeno[2,1-*c*]fluorene (**3a**) [11]. Compound **2a** also exhibited sub-picosecond internal conversion from the S_2 state, that absorbs from 580 nm to 700 nm, to the S_1 state, followed by excited state decay (Figure 2c). Once again, the lower excited state occupies a similar spectral region as the ground state bleach, from approximately 500 nm to 575 nm. The S_1 excited state lifetime of **2a** was $\tau = 9.7 \pm 0.9$ ps (Figure 2d). Vibrational cooling also takes place in **2a**, but again the short lifetimes of all the relaxation processes make it difficult to assign a rate for this process.

In **3a**, unlike **1a** and **2a**, the S_0–S_1 transition is allowed, and thus there is some population in both S_2 and S_1 upon initial excitation at this wavelength. In addition to sub-picosecond internal conversion, a slower blue-shift in the region of 500–600 nm can be assigned a lifetime of $\tau = 1.8$ ps (Figure 2e), which corresponds well to rates of intramolecular vibrational cooling to the lowest excited state observed in many systems [34–36]. This shift was followed by excited state decay in $\tau = 9.5 \pm 1.7$ ps (Figure 2f). Thus, the same S_1 decay behavior was observed in solutions of **1a**, **2a** and **3a**, indicating picosecond excited state decay is common among these derivatives containing de-aromatized quinoidal cores. The related substructure of indenofluorene, *s*-indacene derivative **4**, was found to have lifetimes of $\tau = 18$ ps and $\tau = 2.5$ ps for the S_1 and S_2 states, respectively. The lifetimes of **4** are similar to excited states for the larger systems of this study, indicating a similar relaxation mechanism may be responsible [37–39]. The extremely short ca. 10–20 ps excited state lifetimes explain why **1**–**4** are non-emissive molecules, since fluorescence is not a competitive process at this time scale [40].

We wanted to understand how rapid internal conversion of the excited state to the ground state takes place; thus, we took inspiration from the studies of **4**. It is believed **4** is able to efficiently return to the ground state through a potential energy surface crossing between S_1 and S_0 states [21]. We therefore searched computationally for a conical intersection between the S_1 and S_0 states of **1**–**3**.

Interestingly, TD-DFT calculations using CAM-B3LYP predict a symmetry forbidden $S_0 \rightarrow S_1$ transition for **1b** and **2b**, the compounds containing an inversion center, which is attributed to a HOMO-1 → LUMO transition; however, the $S_0 \rightarrow S_1$ transition is allowed for **3b**, which does not possess an inversion center (see Supporting Information). The smallest active space for exploring the conical intersection was therefore deemed to consist of 4 electrons and 4 orbitals to include the HOMO-1. The FORS(4,4) results for **1b**, **2b**, and **3b** show that the S_1 state differs from the ground state in that the localized double bond character of the central rings becomes attenuated. Here it should be noted that FORS overestimates the energy of the $S_0 \rightarrow S_1$ transition and the $S_0 \rightarrow S_1$ reorganization energy; for example in **3a** the measured $S_0 \rightarrow S_1$ energy is 1.48 eV while that predicted by FORS for **3b** is 3.29 eV. This can be partially remedied by the inclusion of dynamic correlation

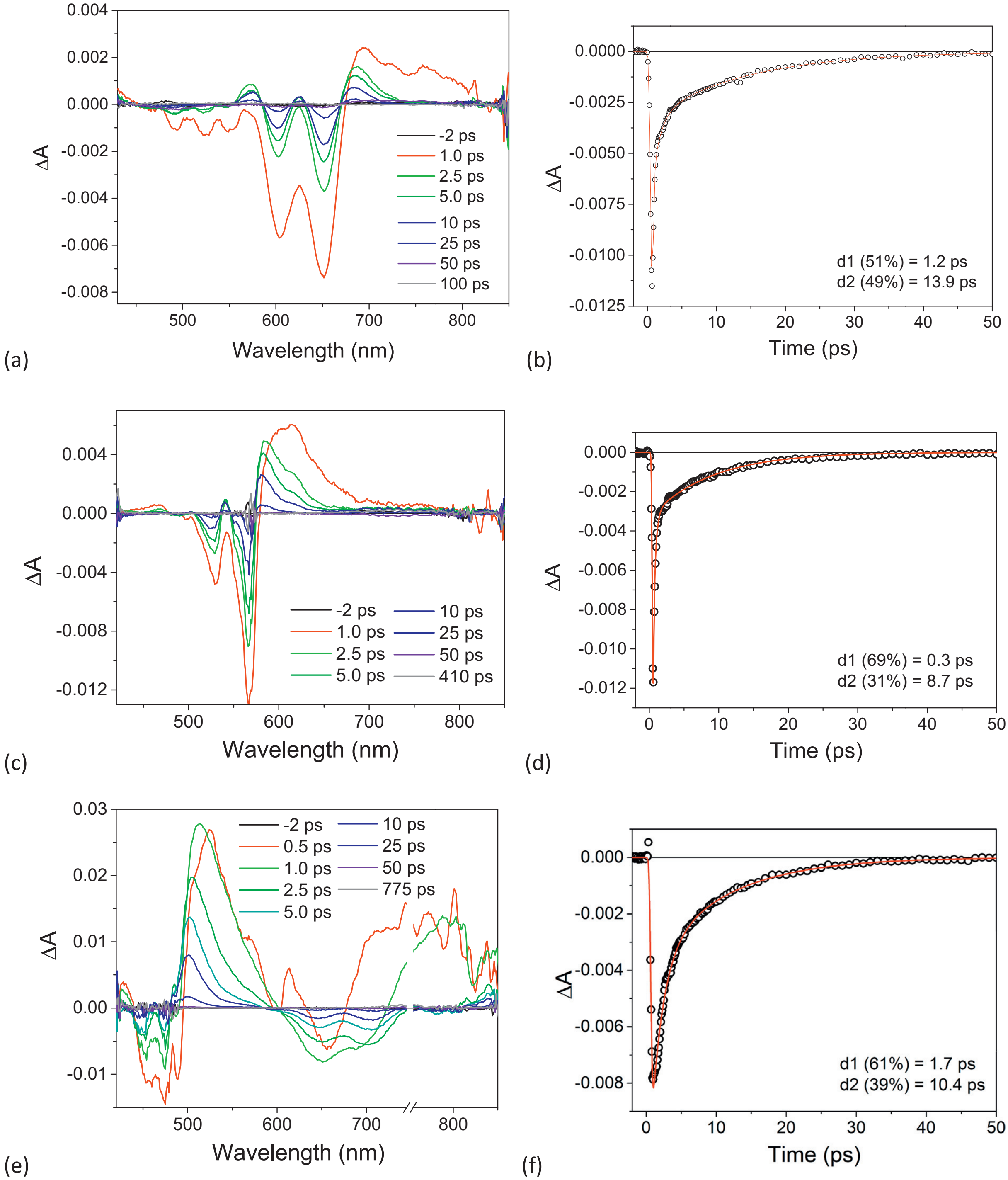

Figure 2. Femtosecond transient absorption spectra and kinetics traces from the ground state bleach in a toluene solution of (a) **1a** at (b) 649 nm, (c) **2a** at (d) 529 nm, and (e) **3a** at (f) 645 nm, showing recovery corresponding to rapid excited state decay pathways.

using MCQDPT2. A SA-MCQDPT2(4,4) single point energy calculation predicts the **3b** vertical $S_0 \rightarrow S_1$ transition to be 2.27 eV (546 nm), closer in alignment with experimental data for **3a** (1.93 eV, 647 nm). The SA-MCQDPT2 $S_0 \rightarrow S_1$ reorganization energies are 0.70 eV for **1b**, 0.68 eV for **2b**, and 0.14 eV for **3b**. Continuing on from the S_1 geometry, only a small perturbation is required to reach the geometry of the conical intersection (Figure 3). This facile S_1-to-conical intersection rearrangement is reflected in the geometries as well as the potential energy surfaces. The energy difference for the S_1 potential energy surface going from the S_1 geometry to the conical intersection is 0.03 eV for **1b**, 0.26 eV for **2b**, and 0.05 eV for **3b**. While qualitative in nature, the small difference in energy and geometry between the S_1 and conical intersection geometry strongly implicates that a conical intersection is the likely mechanism for efficient non-radiative decay to the ground state, similar to **4**.

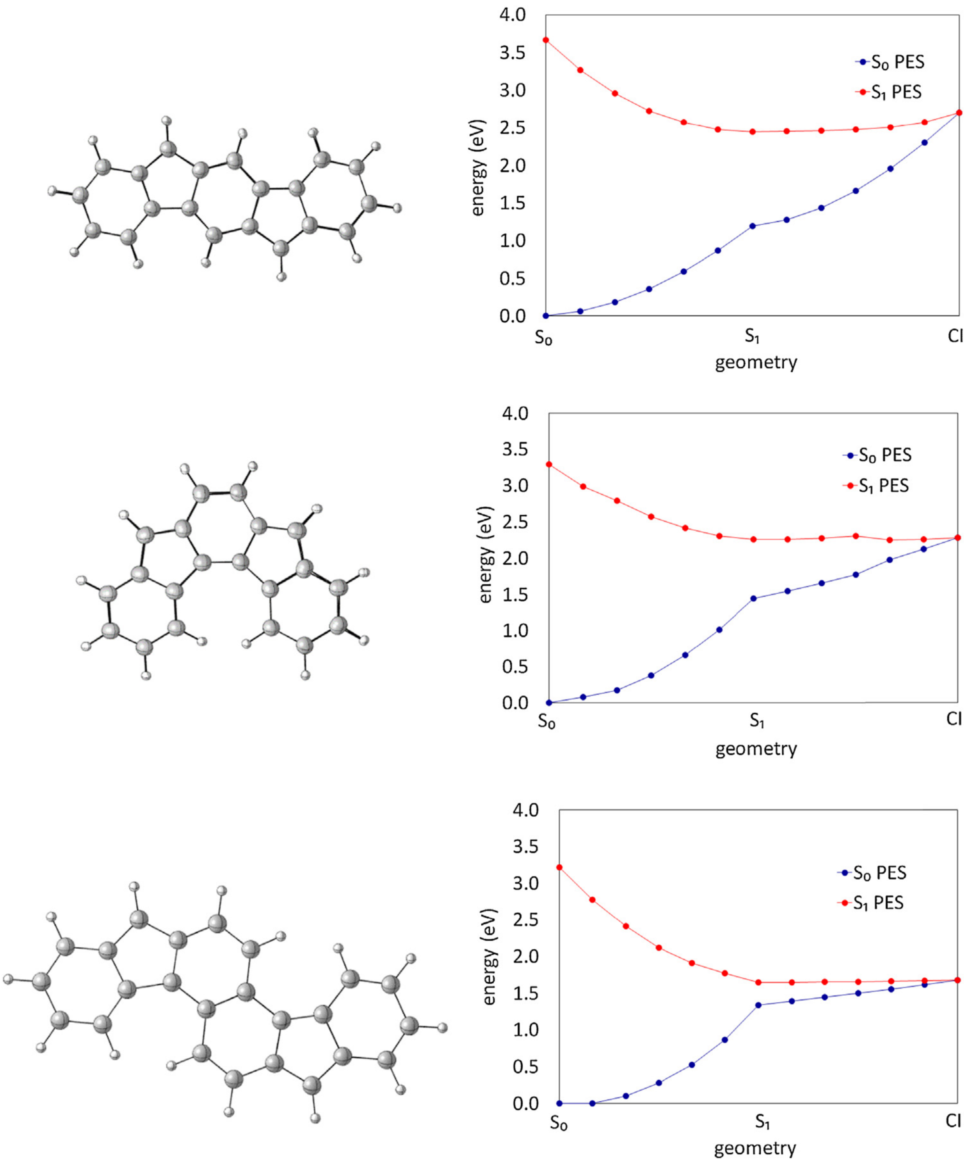

Figure 3. Overlay of SA-FORS(4,4) calculated S_1 and conical intersection geometries (left) and interpolated energies for S_0 and S_1 potential energy surfaces (PES) in vacuum (right) for **2b** (top), **3b** (middle), and **1b** (bottom). The axis labeled geometry indicates the location of the optimized geometry for the S_0 electronic state, S_1 electronic state and conical intersection (CI) in the plot. Five linearly interpolated geometries between the S_0 and S_1 as well as the S_1 and CI are included on the plot.

4. Conclusions

We have reported the solution excited state lifetimes for quinoidal molecules **1a**–**3a** as measured by transient absorption spectroscopy, and computationally explored the S_1/S_0 potential energy surface crossing for simplified models systems **1b**–**3b**. This series of quinoidal molecules was found to have very short S_1 excited state lifetimes (ca. 9–12 ps) due to an easily accessible S_1/S_0 conical intersection. This work helps lay a foundation for future explorations on solid thin films of these molecules and other related pi-conjugated quinoidal compounds.

Acknowledgments

This work was supported by the National Science Foundation (CHE-1301485, M.M.H.) and the Chemical Sciences, Geosciences, and Biosciences Division, Office of Basic Energy Sciences, DOE (DE-FG02-99ER14999, M.R.W.). B.D.R. acknowledges the NSF for a GK-12 fellowship (DGE-0742540). We thank Dr. Johannes Gierschner for valuable initial discussions, Samuel Eaton, Eric Margulies, and Dr. Ryan Young for constructive discussions, and Aaron Fix for supplying compound **3a**.

Appendix A. Supplementary data

Supplementary data associated with this article can be found, in the online version, at doi:10.1016/j.cplett.2014.10.031.

References

[1] S.-S. Sun, L.R. Dalton (Eds.), Introduction to Organic Electronic and Optoelectronic Materials and Devices, CRC Press, Boca Raton, FL, 2008.
[2] S.R. Forrest, Nature 428 (2004) 911.
[3] E. Wang, W. Mammo, M.R. Andersson, Adv. Mater. 26 (2014) 1801.
[4] C.D. Dimitrakopoulos, P.R.L. Malenfant, Adv. Mater. 14 (2002) 99.
[5] M. Bendikov, F. Wudl, D.F. Perepichka, Chem. Rev. 104 (2004) 4891.
[6] J. Huang, J.-H. Su, H. Tian, J. Mater. Chem. 22 (2012) 10977.
[7] D. Chen, et al., Org. Electron. 15 (2014) 1197.
[8] S. Karak, V.S. Reddy, S.K. Ray, A. Dhar, Org. Electron. 10 (2009) 1006.
[9] M. Heeney, et al., Macromolecules 37 (2004) 5250.
[10] B.D. Rose, C.L. Vonnegut, L.N. Zakharov, M.M. Haley, Org. Lett. 14 (2012) 2426.

[11] A.G. Fix, P.E. Deal, C.L. Vonnegut, B.D. Rose, L.N. Zakharov, M.M. Haley, Org. Lett. 15 (2013) 1362.
[12] D.T. Chase, et al., J. Am. Chem. Soc. 134 (2012) 10349.
[13] D.T. Chase, et al., Angew. Chem. Int. Ed. 50 (2011) 11103.
[14] B.D. Rose, et al., J. Am. Chem. Soc. 136 (2014) 9181.
[15] A. Shimizu, Y. Tobe, Angew. Chem. Int. Ed. 50 (2011) 6906.
[16] M.J. Kendrick, et al., J. Phys. Chem. C 116 (2012) 18108.
[17] J. Nishida, S. Tsukaguchi, Y. Yamashita, Chem. Eur. J. 18 (2012) 8964.
[18] S. Ito, T. Minami, M. Nakano, J. Phys. Chem. C 116 (2012) 19729.
[19] S.W. Eaton, et al., J. Am. Chem. Soc. 135 (2013) 14701.
[20] M.C. Hanna, A.J. Nozik, J. Appl. Phys. 100 (2006) 074510/1.
[21] M.J. Bearpark, P. Celani, F. Jolibois, M. Olivucci, M.A. Robb, F. Bernardi, Mol. Phys. 96 (1999) 645.
[22] R.F. Kelley, R.H. Goldsmith, M.R. Wasielewski, J. Am. Chem. Soc. 129 (2007) 6384.
[23] J.E. Bullock, et al., J. Phys. Chem. B 114 (2010) 1794.
[24] A.S. Lukas, S.E. Miller, M.R. Wasielewski, J. Phys. Chem. B 104 (2000) 931.
[25] M.W. Schmidt, et al., J. Comput. Chem. 14 (1993) 1347.
[26] H. Nakano, J. Chem. Phys. 99 (1993) 7983.
[27] T.H. Dunning Jr., J. Chem. Phys. 90 (1989) 1007.
[28] R. Krishnan, J.S. Binkley, R. Seeger, J.A. Pople, J. Chem. Phys. 72 (1980) 650.
[29] T. Yanai, D.P. Tew, N.C. Handy, Chem. Phys. Lett. 393 (2004) 51.
[30] Y. Tawada, T. Tsuneda, S. Yanagisawa, T. Yanai, K. Hirao, J. Chem. Phys. 120 (2004) 8425.
[31] B.M. Bode, M.S. Gordon, J. Mol. Graph. Model. 16 (1998) 133.
[32] G. Zhurko, Chemcraft, http://www.chemcraftprog.com
[33] C. Legault, CYLview, Université de Sherbrooke, 2009 http://www.cylview.org
[34] A. Pigliucci, G. Duvanel, L.M.L. Daku, E. Vauthey, J. Phys. Chem. A 111 (2007) 6135.
[35] D. Schwarzer, C. Hanisch, P. Kutne, J. Troe, J. Phys. Chem. A 106 (2002) 8019.
[36] T. Elsaesser, W. Kaiser, Annu. Rev. Phys. Chem. 42 (1991) 83.
[37] R. Klann, R.J. Bäuerle, F. Laermer, T. Elsaesser, M. Niemeyer, W. Lüttke, Chem. Phys. Lett. 169 (1990) 172.
[38] C. Gellini, P.R. Salvi, K. Hafner, J. Phys. Chem. 97 (1993) 8152.
[39] C. Gellini, L. Angeloni, P.R. Salvi, G. Marconi, J. Phys. Chem. 99 (1995) 85.
[40] N. Turro, V. Ramamurthy, J. Scaiano, Modern Molecular Photochemistry of Organic Molecules, University Science Books, Sausalito, CA, 2010.